Available online at www.sciencedirect.com
ScienceDirect
Physics Procedia 5 (2010) 595–606
Physics Procedia
www.elsevier.com/locate/procedia

LANE 2010

Additive manufactured Ti-6Al-4V using welding wire: comparison of laser and arc beam deposition and evaluation with respect to aerospace material specifications

E. Brandl[a]*, B. Baufeld[b], C. Leyens[c], R. Gault[d]

[a]EADS Innovation Works, Metallic Technologies & Surface Engineering, D-81663 Munich, Germany
[b]Katholieke Universiteit Leuven, Department of Metallurgy and Materials Engineering Kasteelpark Arenberg 44, B-3001 Leuven, Belgium
[c]Technische Universität Dresden, Institute of Materials Science, Helmholtzstr. 7, D-01062 Dresden, Germany
[d]University of Sheffield, Advanced Manufacturing Park, Wallis Way Catcliffe, Rotherham S60 5TZ, United Kingdom

Abstract

In this paper, the results of two different wire based additive-layer-manufacturing systems are compared: in one system Ti-6Al-4V is deposited by a Nd:YAG laser beam, in the other by an arc beam (tungsten inert gas process). Mechanical properties of the deposits and of plate material are presented and evaluated with respect to aerospace material specifications. The mechanical tests including static tension and high cycle fatigue were performed in as-built, stress-relieved and annealed conditions.
Generally, the mechanical properties of the components are competitive to cast and even wrought material properties and can attain properties suitable for space or aerospace applications.

Keywords: additive layer manufacturing; wire; titanium; Ti-6Al-4V; laser; arc beam; shape metal deposition; rapid manufacturing

1. Introduction

Techniques for building up geometries layer by layer, generally referred to as rapid prototyping, have proved to be very effective in accelerating product development and thus reducing time to market with respect to traditional machining approaches. Understandably, these techniques have been increasingly successful since their introduction in 1986 [1]. Several techniques, such as stereolithography or selective sintering/melting, have been developed and successfully commercialized in the industry under numerous trade names, e.g. Direct Manufacturing, Direct Laser Fabrication, Freeform Fabrication, or Selective Laser Melting. Due to the speed of development different terms have been created which are generally not clearly defined or differentiated [2]. All of these techniques, however, share the layer additive approach, and so are often referred to as additive layer manufacturing (ALM).

Nowadays, not only are prototypes realized by using these techniques, but also serial production parts are envisaged [3,4], which is referred to as rapid manufacturing. To achieve this progress, development activities have to improve both reliability and output material quality. Material quality is an all-important factor, particularly for

* Corresponding author. Tel.: +49-89-607-22107; fax: +49-89-607-25408.
E-mail address: erhard.brandl@eads.net.

1875-3892
doi:10.1016/j.phpro.2010.08.087

aerospace applications. In this paper, the material investigated is the titanium alloy Ti-6Al-4V, the most commonly produced titanium alloy and one of the most common aerospace alloys [5-7].

Nearly all additive manufactured Ti-6Al-4V parts are built from powderized feedstock in either a powder-bed or powder-feed process [3]. Wire-feed processes have received less attention, as the development has been concentrated on eye-catching and complex geometries rather than on deposition speed, efficiency, or material quality. The increasing market demand for Ti-6Al-4V serial production parts has promoted wire-feed processes, as material properties, possible part size, and building speed have also become issues.

This paper aims to increase the knowledge regarding material properties. Two different wire-feed based systems are compared: in one system Ti-6Al-4V is deposited by a Nd:YAG laser beam, in the other by an arc beam (tungsten inert gas process), also known as shaped metal deposition (SMD). Mechanical properties of the deposits and of plate material are presented and evaluated from an aerospace point of view. The mechanical tests including static tension and high cycle fatigue were performed in as-built, stress-relieved and annealed conditions.

2. Experimental details

2.1. Wire based additive layer manufacturing

Two wire-feed processes are investigated: The process using a laser beam is abbreviated to WF-L-Beam, the SMD process using an arc beam to WF-A-Beam.

2.1.1. Laser beam based deposition (WF-L-Beam)

The experimental setup essentially comprises a Trumpf HLD 3504 Nd:YAG rod laser (diode pumped) with a maximum power of 3.5 kW, a Weldaix wirefeeder and a Kuka KR 100 HA (high accuracy) 6-axis robot. In an open box, which is permanently flooded by argon from its base (design of the box based on [8]), Ti-6Al-4V welding wire is deposited onto a Ti-6Al-4V substrate. An overview of the setup, a schematic drawing of the process, and exemplary components are shown in Fig. 1. The setup was developed at EADS Innovation Works in Ottobrunn/Munich (Germany).

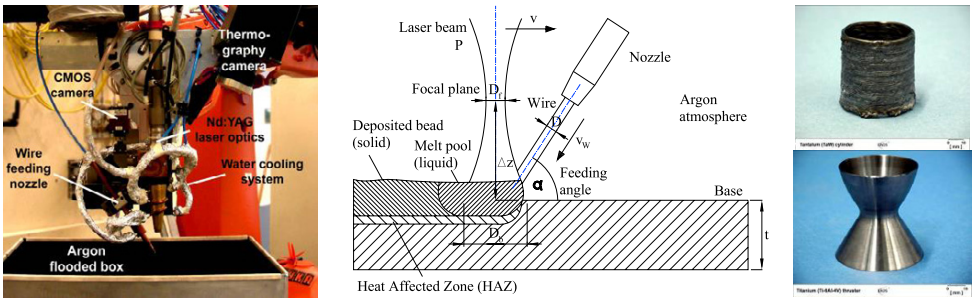

Fig. 1. (a) Experimental setup of the WF-L-Beam process; (b) Schematic drawing of the process; (c) Exemplary components: Ta-20W cylinder (as-built surface) and Ti-6Al-4V thruster (machined surface)

The best performance in terms of surface finish, dimension control and bead quality was obtained by front-feeding and placing wire at the leading edge of the melt pool, which is in agreement with several publications dealing with improving the wire-feed deposition process [9-14]. Details of the experimental settings are listed in Table 1.

Table 1. Details of the WF-L-Beam process

	Abbreviation	Unit	Dimension
Laser power	P	[kW]	1.75 – 3.5
Diameter of optical fibre		[mm]	0.4
Focal length of optics		[mm]	140.0
Focal plane diameter	D_f	[mm]	0.56
Focal position	Δz	[mm]	23
Diameter of beam at plate surface	D_b	[mm]	~ 4.1
Thickness of Ti-6Al-4V base	t	[mm]	6.35
Diameter of Ti-6Al-4V wire	D	[mm]	1.2
Feeding angle	α	[°]	55
Deposition or welding speed	v	[mm/s]	7.5 – 40
Wire-feed speed	v_W	[mm/s]	k * v = 15 – 160
Wire-feed speed factor	k	[1]	$k = v_W / v = 2 – 5$

2.1.2. Arc beam based deposition (WF-A-Beam)

The WF-A-Beam samples were produced by the shaped metal deposition (SMD) process at the Advanced Manufacturing Research Centre (AMRC) in Sheffield (UK). The company Rolls-Royce has developed the process originally and has several patent applications pending [15-24]. The process has been further developed at the AMRC. It is basically a tungsten inert gas welding process. The SMD cell consists of a welding torch attached to a 6-axis Kuka robot linked to a 2-axis table. The setup is enclosed in an airtight chamber filled with argon. Further details of the process can be found in [25-28] and details of material properties in [27-32]. Examples of differently shaped components are shown in Fig. 2.

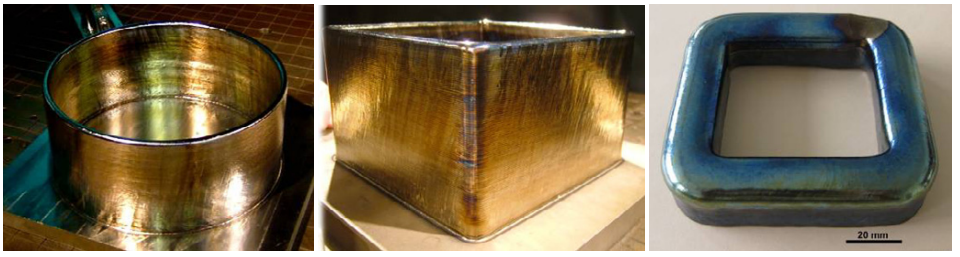

Fig. 2. Ti-6Al-4V components built by WF-A-Beam (Shape Metal Deposition)

2.2. Post build-up heat treatments

Two post build-up heat treatments, typical for Ti-6Al-4V parts used in aerospace, were applied:

- Stress-relieving at 600°C for 4 h in vacuum (10^{-4} - 10^{-5} mbar) followed by furnace cooling (FC) [33] to reduce residual stresses without substantial change to microstructure [34]. Stress-relieving is generally recommended after welding [35]. The treatment of 600°C for 4 h can also be considered as an aging treatment [33,34] to produce precipitates resulting in an increase in strength, which can be applied to solution-treated and water-quenched material [34].
- Annealing at 834°C for 2 h in vacuum (10^{-4} - 10^{-5} mbar) followed by furnace cooling [33,36,37] to eliminate a strength increase or develop a stable temper [34].

Heat treatments were carried out before final machining of the samples to prevent contamination from the atmosphere.

2.3. Mechanical characterization

Static tensile tests were performed on a Z250 (Zwick) at room temperature according to EN 10002 [38]. The designation, shape and test velocity of the samples used are illustrated in Table 2.

Table 2. Static tensile sample (dimensions in [mm])

Design	Test velocity	Drawing
EADS	0.4 mm/min	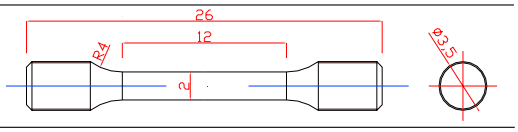

High cycle fatigue (HCF) samples (Table 3) were tested according to DIN 50100 [39] at room temperature on a Microtron 654 (Rumul) resonance tester. A test frequency of approximately 100 Hz and a load ratio of R = 0.1 were used. The stress concentration factor is approximately $\alpha_K = 1$. Tests were terminated at $4 \cdot 10^7$ cycles. All samples were electrochemically polished (~60 µm diameter reduction) to remove potential residual stresses and hardening effects at the surface, which result from machining/milling [40] and would cause erroneous cycle fatigue results [41,42].

Table 3. High cycle fatigue sample (dimensions in [mm])

Design	Test frequency	Drawing
EADS	~ 100 Hz	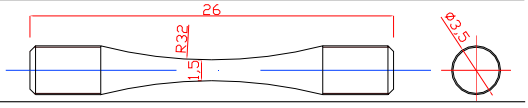

2.4. Sample manufacturing

2.4.1. WF-L-Beam builds

The building strategy, sample extraction, and designation of the WF-L-Beam builds are shown in Figure 3.

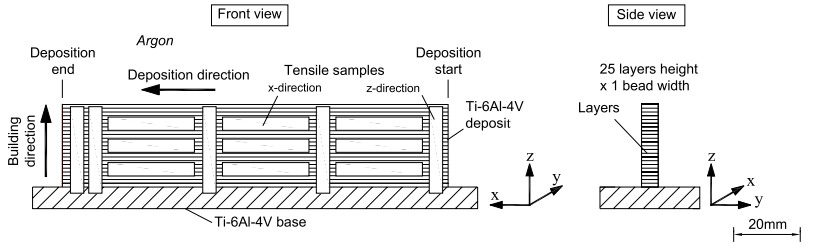

Fig. 3. Building strategy, sample extraction and designation of directions at WF-L-Beam builds (25 layers x 1 bead)

Samples were extracted from several walls (25 layers high by 1 bead wide) whose wall width was about 4 - 5 mm. All geometries were built by adopting a single deposition direction. After each layer deposited, the z-

coordinate of the deposition head was increased. Suitable z-increments at certain parameter sets have been published in [43]. The process was paused between these layers until the temperature of the previous layer fell below 300°C. The samples were extracted at different locations and from different directions. The location of sample extractions was randomized in order not to test material from only one region of the build for any given treatment. The samples that were post heat treated were also chosen in a randomized way. As shown in Fig. 5, hardness varies significantly between different points of the wall and varying mechanical properties are expected. Randomization ensures that these effects are balanced and properties are averaged. The samples are labeled as x when they are extracted parallel to the deposition direction and as z when they are parallel to the building direction, i.e. perpendicular to the layers.

The process parameters used for the builds are a laser power P = 2625 W, z increment Δz = 0.95 mm, welding speed v = 7.5 mm/s, and a wire-feed speed v_W = 30 mm/s, i.e. a wire-feed speed factor k = v_W/v = 4.

2.4.2. WF-A-Beam build

The WF-A-Beam samples were extracted from a 75 layers x 1 bead build in the form of a square based tubular component with wall width of 9 mm and side lengths of 275 mm. The building strategy shown in Fig. 4 is comparable to the WF-L-Beam build (Fig. 3). As with WF-L-Beam samples, the post build-up heat treatment of the WF-A-Beam samples was randomized in order to balance location effects and average mechanical properties.

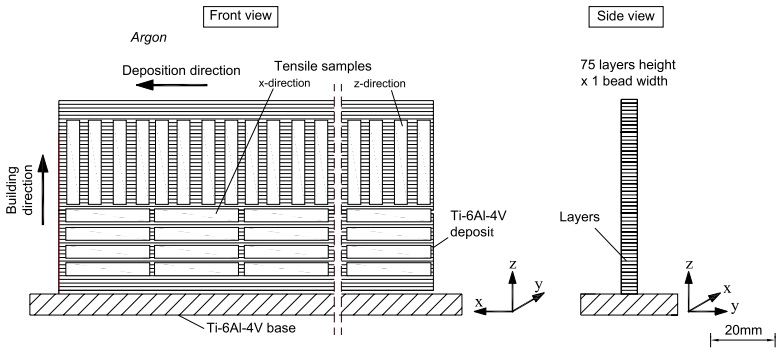

Fig. 4. Building strategy, sample extraction and designation of directions at the WF-A-Beam build (75 layers x 1 bead)

The build was produced in the frame of the RAPOLAC project [25]. The process parameters used are a welding current I = 176.8 A, voltage U = 12.4 V, z increment Δz = 1 mm, welding speed v = 5 mm/s, and a wire-feed speed v_W = 33.3 mm/s, i.e. a wire-feed speed factor k = v_W/v = 6.67.

3. Results

The results in this paper are focused on mechanical properties which are complemented by hardness measurements. The microstructure and morphology of builds produced by WF-L-Beam are published in [43-45] and of WF-A-Beam builds in [27-30].

3.1. Hardness

The hardness distributions and average hardness of WF-L-Beam walls (y-z plane) in the as-built and 843°C/2h/FC condition are shown in Fig. 5. The average hardness of the wire and of the plate material is shown as well.

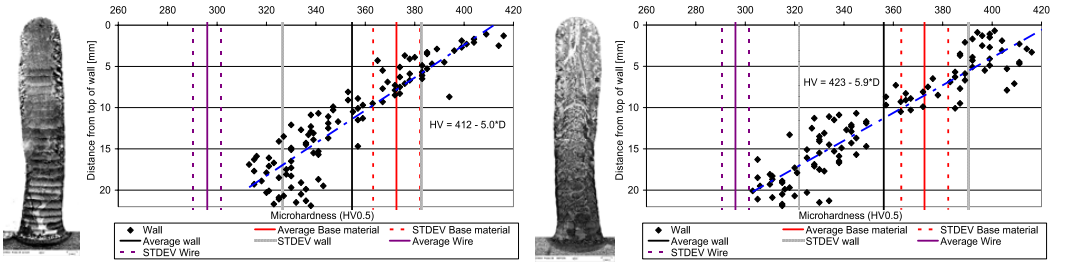

Fig. 5. Morphology and corresponding hardness profile (y-z plane) of 25 layers x 1 bead build produced by WF-L-Beam in (a) as-built condition; (b) 843°C/2h/FC condition

The average hardness of WF-L-Beam walls is 355 ± 28 HV0.5 in the as-built condition, and 356 ± 34 HV0.5 in the 843°C/2h/FC condition. This hardness decreases considerably with increasing distance from the top, being slightly steeper in the 843°C/2h/FC condition (-5.9 HV0.5/mm) than in the as-built condition (-5.0 HV0.5/mm). For the WF-A-Beam not such a steep relation of the hardness in dependence on the height was observed decreasing from 346 ± 16 HV0.1 within the top 10 mm to 337 ± 14 HV0.1 in the center of the build. After annealing the hardness was 335 ± 16 HV0.1, indicating that, similar to the situation for the WF-L-Beam, annealing at 843°C does not affect the hardness.

3.2. Static tensile properties

3.2.1. WF-L-Beam builds

Depending on post build-up heat treatment and test direction, the average values of yield strength reaches 791 – 874 MPa, ultimate tensile strength 872 – 940 MPa, elongation 4.1 – 12.5 %, and reduction of area 19.8 – 45.3 %. The plate material reaches an average yield strength of 922 MPa, ultimate tensile strength of 984 MPa, elongation of 15.1 %, reduction of area of 32.2 %. Fig. 6a shows these strength and Fig. 6b these ductility properties.

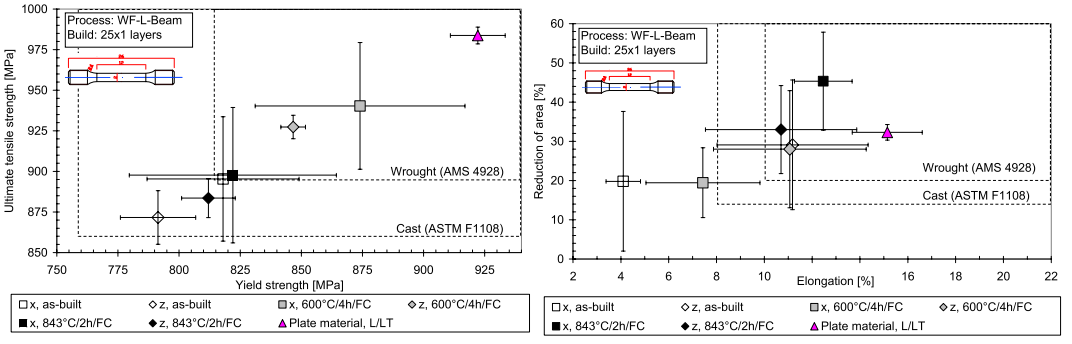

Fig. 6. (a) Yield and ultimate tensile strength, (b) elongation and reduction of area of as-built, 600°C/4h/FC, and 843°C/2h/FC material built by WF-L-Beam, tested along (x) and across (z) deposition direction in comparison with base material used, wrought [46], and cast material [47]; one data point represents the average of 3-5 WF-L-Beam and 6 plate (3 L, 3 LT direction) samples tested and error bars indicate standard deviation

As can be seen in Fig. 6, 2 out of the 6 WF-L-Beam batches tested achieve both strength and ductility properties of wrought material, and 4 achieve at least both strength and ductility properties of cast material.

The following important findings can be derived:

- Samples tested in x-direction show higher strength and, except in the case of the 843°C/2h/FC condition, considerably lower ductility than those tested in z-direction.

- The 600°C/4h/FC treatment increased strength considerably in comparison to the as-built condition.
- The 843°C/2h/FC treatment considerably increased ductility in x-direction in comparison to the as-built condition, and tend to increase the strength slightly.

3.2.2. WF-A-Beam builds

Fig. 7 shows the strength and ductility data of WF-A-Beam samples. Depending on post build-up heat treatment and test direction, the average values of yield strength reaches 856- 915 MPa, ultimate tensile strength 930 – 981 MPa, elongation 6.6 – 20.5 %, and reduction of area 12.8 – 50.0 %.

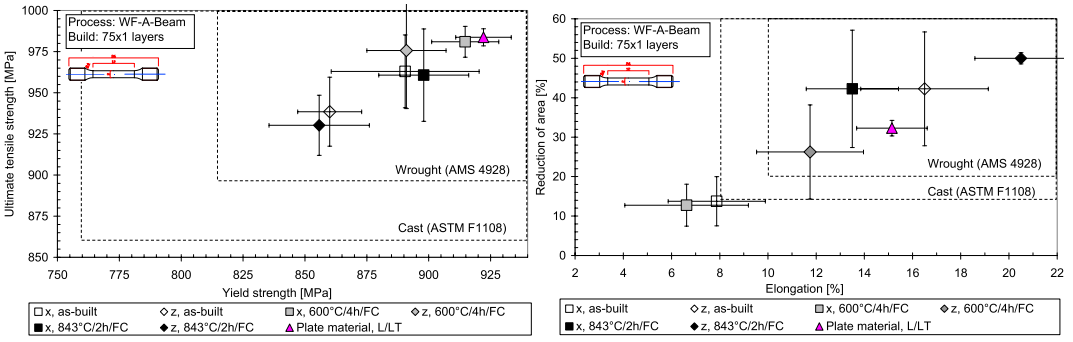

Fig. 7. (a) Yield and ultimate tensile strength, (b) elongation and reduction of area of as-built, 600°C/4h/FC, and 843°C/2h/FC material built by WF-A-Beam, tested along (x) and across (z) deposition direction in comparison with plate, wrought [46], and cast material [47]; one data point represents the average of 4 WF-A-Beam and 6 plate (3 L, 3 LT direction) samples tested and error bars indicate standard deviation

As can be seen in Fig. 7, 4 out of 6 WF-A-Beam batches tested achieve the properties of wrought material and the remaining 2 show ductility properties below that of cast material. All 843°C/2h/FC samples and all z-samples show wrought material properties. The following findings can be derived:

- Samples tested in x-direction show higher strength and considerably lower ductility than those tested in z-direction.
- The 600°C/4h/FC treatment increased strength and reduced ductility in comparison to the as-built condition.
- The 843°C/2h/FC treatment increased ductility in comparison to the as-built condition, while not largely affecting strength comparative to the as-built condition. After this heat treatment the elastic properties in z-direction exceed the one of the plate material by far.

3.3. High cycle fatigue (HCF) properties

Fig. 8 shows the high cycle fatigue properties of 843°C/2h/FC WF-L-Beam and as-built and 843°C/2h/FC WF-A-Beam material respectively. The samples were tested in x- and z-direction. Samples of the plate material used (longitudinal-direction) are tested for comparison.

The applicable range of maximum stress was narrow: An upper limit is set by yield strength (see Fig. 6a and Fig. 6b) as plastic deformation should be avoided in HCF tests [39]. The lower limit is set high, at approximately 760 MPa (WF-L-Beam) and 780 MPa (WF-A-Beam), as samples ran out below this stress. The material therefore did not show typical Wöhler curve behaviour.

Due to the scattering of the WF-L-Beam material, a fatigue limit is difficult to determine, but it tends to be higher than 700 MPa for the most batches tested, and thus higher than of wrought material. The material tends to have higher dynamic strength in x-direction than in z-direction.

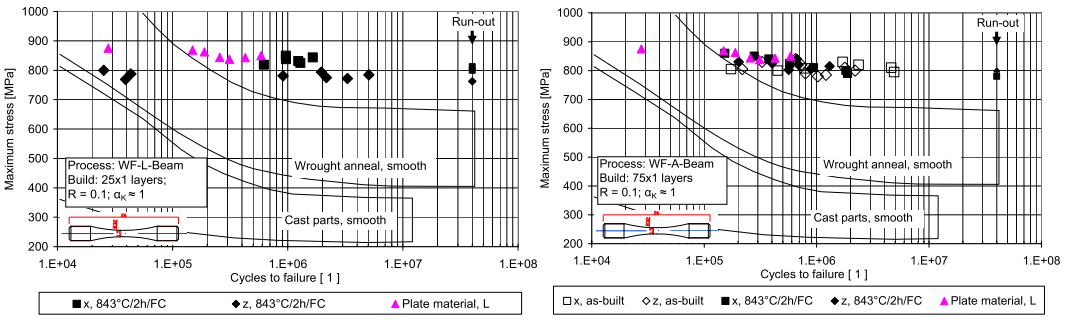

Fig. 8. High cycle fatigue properties of (a) WF-L-Beam and (b) WF-A-Beam material, tested along (x) and across (z) deposition direction in comparison with plate material used, wrought, and cast material [48]; one data point represents one sample tested

The WF-A-Beam material shows an agglomeration of data points in the area between $2 \cdot 10^5$ - $2 \cdot 10^6$ cycles and 780 - 860 MPa. The possible stress range was even narrower than for the WF-L-Beam samples. The determination of a fatigue limit is, in this case, not meaningful, but the dynamic strength is approximately comparable to the plate material tested. The material tends to have a similar dynamic strength in the as-built and 843°C/2h/FC condition. The dynamic strength of material tested in x-direction is similar to that tested in z-direction. Early failure at cycle numbers smaller than $5 \cdot 10^4$ like for the WF-L-Beam samples was not observed for the WF-A-Beam samples.

4. Discussion

The material manufactured by wire-feed additive layer manufacturing can attain static tensile properties of the material specifications AMS 4928 [46] of wrought material and/or ASTM F1108 [47] of cast material. It also reaches or exceeds fatigue properties of wrought anneal, smooth material [48], while the small size of the samples (Table 3) may contribute to the high fatigue limit (size effect) [49].

The manufacturing technology is therefore an interesting alternative for the manufacture of space and aerospace components. The properties, however, should be adapted to the specific application by suitable post heat treatment and load direction. Some important experimental findings are further discussed in the following.

It was observed that for both ALM techniques the average hardness is approximately similar in the as-built and in the 843°C/2h/FC condition.

In terms of the 843°C/2h/FC treatment, there are two competing effects regarding hardness. On the one hand, the α-lamellae grow and martensitic microstructures dissolute into fine lamellar α+β microstructures [50]. Hardness decreases due to reduced number of boundaries and/or dislocations in the microstructure [50]. Not only numerous boundaries, but also a high dislocation density is produced when α+β-alloys are cooled at high rates from the β-phase field [50]. The α-content, however, increases and approaches equilibrium phase distribution. As the β-phase is softer than α, hardness increases when the phase distribution approaches equilibrium (~95 % α, ~5 % β) [51]. Hence, this could explain why the hardness values are similar in the as-built and 843°C/2h/FC conditions. The hardness properties are in line with those of strength (see Fig. 6a and Fig. 7a), which is also not significantly affected by a 843°C/2h/FC treatment.

A further finding is that the 600°C/4h/FC treatment tends to increase strength in WF-L-Beam and WF-A-Beam material compared to the as-built condition. In WF-A-Beam material, the ductility decreases after 600°C/4h/FC treatment.

With respect to the hardening mechanisms [48,50], it is suggested that the 600°C/4h/FC treatment leads to Ti_3Al precipitation hardening, which consequently increases yield strength [50]. Indeed, as described in [48,50,52], precipitation hardening of the α-phase occurs by coherent Ti_3Al (α_2) particles. Upon annealing in the α+β-region, significant alloy element partitioning takes place and the α-phase is enriched in α-stabilizing elements (Al, O, Sn) and substantial volume fractions of coherent Ti_3Al particles can be precipitated in the α-phase by aging, for

example, at 500°C (Ti-6Al-4V) [50]. In [48], aging temperatures of 500 - 600°C are reported by Ti-6Al-4V containing less than 0.2 wt.% oxygen. At high aging temperatures, ordering should not be expected, as oxygen would have a high jump frequency. In contrast, it is noted in [50] that the Ti_3Al solvus temperature is approximately 550°C and a heat treatment at 600°C or above would be only a stress relieving treatment. The further typical aging temperatures found in literature are mostly below 600°C, e.g. in [53] at which Ti_3Al precipitation was observed after a 540°C/2h treatment. Nevertheless, according to [54], Ti_3Al precipitation is slow and the influence of cooling speed is strong. Fast cooling after aging leads to more strength loss than slow furnace cooling. For maximum strength, slow furnace cooling to 400°C is required [54]. Therefore, during the slow heating and furnace cooling applied by the 600°C/4h/FC treatment, the material is, at least for a certain time, in the temperature region of precipitation hardening, which would explain the increased strength properties observed.

The strengthening effect due to aging of various lamellar Ti-6Al-4V microstructures can be seen in [55]. Ti-6Al-4V is heated to four different temperatures ($T \geq T_\beta$, $M_S < T < T_\beta$, $T \geq M_S$, $T < M_S$) and cooled at three different rates (water quenched, air cooled, and furnace cooled). The mechanical properties show that in 9 out of these 12 cases a subsequent aging treatment at 538°C/4h/FC increased strength. Additionally, in 9 cases, ductility decreased after aging. According to [50], Ti_3Al precipitation not only increases yield strength, but also reduces elongation at failure. This could explain the ductility loss at WF-A-Beam material.

It was found out that the 843°C/2h/FC treatment tends to increase ductility in WF-L-Beam (x-direction) and WF-A-Beam material, while not significantly affecting strength comparative to the as-built condition.

There are two competing effects regarding strength. Due to the 843°C/2h/FC treatment, the microstructure coarsened, i.e. the α-lamellae grew due to heat input. The mean self-diffusion length of titanium after 2 h at 843°C is about 0.4 µm (calculated by $x = \sqrt{(2Dt)}$ [56] and Arrhenius diagram in [57]) which is about half of the α-lamella width in the as-built condition (see [44]). Furthermore, martensitic microstructures change into fine lamellar α+β microstructures, annealing them in the temperature region of 700 - 850°C [50]. These factors cause strength to decrease due to loss of martensite, boundaries and/or dislocations, and ductility increases due to reduced martensite and dislocations [50,58]. By contrast, however, α-content increases and approaches equilibrium phase distribution. The α-phase is harder than the β-phase, and strength increases if the α-content is increased [51,59]. In summary, strength properties are not largely affected, which is probably due to these competing effects, although ductility is increased.

WF-L-Beam and WF-A-Beam material tested in x-direction tends to have a higher strength, and lower ductility than tested in z-direction. WF-L-Beam material tends to have a slightly higher dynamic strength in x-direction than in z-direction.

Generally, anisotropic mechanical properties are expected here, due to anisotropic microstructure (see [30,43]). The morphology of WF-L-Beam and WF-A-Beam builds consists of columnar, prior β-grains which grow across many layers in counter direction to the heat flux (i.e. in the building direction), which is described in [43,45] and [27-30] respectively. These prior β-grains contain a lamellar α+β microstructure. Regarding static and dynamic strength, the effective grain size of prior β-grains is smaller in the direction perpendicular to the columnar grains than parallel to the grains [28,60]. A smaller grain size increases static and dynamic strength [50]. Nevertheless, a finer grain size should also increase elongation [50], which is not commonly observed in the tests. With the WF-A-Beam material a possible cause of lower ductility in x-direction was suggested in [28], grain boundaries being potential points of failure. However, the mechanical properties are considered to be dominantly influenced by the much reduced size of the α-lamellae than of prior β-grains. In material produced by a electron beam based powder-bed process [61], the microstructural investigations were wide-ranging and it is reported that, in xy-direction, colony size is more evenly distributed and smaller than in z-direction. Small differences such as the latter one may possibly explain mechanical differences. Additionally, another reasonable explanation for anisotropic strength and ductility may be the anisotropy of crystallographic texture [62]. Regarding textures, one can imagine the direction of the beads as comparable to a rolling or extrusion direction, i.e. the longitudinal direction. The longitudinal direction is parallel to the principal direction of flow in worked metal [63] and typically shows higher strength properties [64] than the transversal or short transverse direction, as the grains and defects are parallel aligned. However, the effect of texture on properties is not straightforward. Further investigations on SMD material can be found elsewhere [65].

It was observed that WF-A-Beam material tends to have a similar dynamic strength in the as-built and 843°C/2h/FC condition and its dynamic strength tested in x-direction is similar to that tested in z-direction.

As the static strength of WF-A-Beam material is not largely affected by the 843°C/2h/FC treatment, HCF strength is also not expected to be largely affected according to [48,50]. Unlike WF-L-Beam material [43-45], WF-A-Beam material does not contain martensite [27,28] that is transformed into α+β during a 843°C/2h/FC treatment, and would decrease HCF strength.

As described above, the static strength of WF-A-Beam material tends to be higher in x-direction than in z-direction. The HCF strength in x-direction is therefore expected to be higher, as is the case with WF-L-Beam material. Fatigue strength includes two factors, crack initiation (nucleation) and crack propagation resistance. While crack initiation resistance, often taken as a measure of HCF strength [50,66], is increased in x-direction due to higher number of (prior β-) grain boundaries, crack propagation resistance in x-direction is decreased [48,57]. The latter may be decisive for HCF strength in x-direction being at the same level as in z-direction. At this point, the question arises of why this is not the case with WF-L-Beam material. The HCF strength of WF-L-Beam material in x-direction is higher than in z-direction. The reason is considered to be the amount of the grain boundary α. Cracks can easily propagate along the grain boundary, and a thicker grain boundary α enhances the propagation of cracks along grain boundary [67]. As the WF-L-Beam samples show less (and no continuous) grain boundary α than in the WF-A-Beam material [27,28], the HCF strength in x-direction is probably not decreased to such an extent as to reach the same level as z-direction. Finally, it should be noted that, according to [62,68], essentially no correlation between static and fatigue strength is considered to exist.

5. Conclusion

Depending on process parameters, load-direction, and post build-up heat treatment, the mechanical properties of additive layer manufactured materials vary greatly. Strength and ductility can reach properties comparable to those of cast and wrought material. In some cases ductility is inferior to those of cast material. For both additive layer manufacturing techniques, the dynamic strength of wire-feed material generally exceeds the properties of wrought material. A 843°C/2h/FC treatment increases ductility and a 600°C/4h/FC treatment increases strength. The material tested in building direction (z) generally has higher ductility and lower strength than in deposition direction (x). In general, additive layer manufactured builds can attain properties suitable for space or aerospace applications. The laser and the arc beam processes result in components with comparable properties. Depending on the emphasis on certain properties also the cost and stability of the respective technique will be decisive for future applications. The substitution of presently cast parts may be beneficial applications. The properties, however, should be adapted to the specific application.

Acknowledgements

The activities at EADS Innovation Works were especially supported by Frank Palm, Achim Schoberth, Dr. Claudio Dalle Donne, Pascal Sauer, Josef Willert, Christian Plander, Dieter Meixner, and Vitus Holzinger. The SMD research is performed within the RAPOLAC STREP project under contract number 030953 of the 6th Framework Programme of the European Commission (www.RAPOLAC.eu), which is gratefully acknowledged.

References

[1] D.-S. Choi, S.H. Lee, B.S. Shin, et al., "Development of a direct metal freeform fabrication technique using CO_2 laser welding and milling technology", *J. Mat. Proc. Techn.*, vol. 113, pp. 273-279, 2001

[2] Verein deutscher Ingenieure, "Generative Fertigungsverfahren: Rapid Technologien (Rapid Prototyping): Grundlagen, Begriffe, Qualitätskenngrößen, Liefervereinbarungen", VDI 3404 (Entwurf), 2007

[3] T.T. Wohlers, *Wohlers report 2009: state of the industry,* Fort Collins, Colorado, Wohlers Associates, 2009

[4] E.C. Santos, M. Shiomi, K. Osakada, et al., "Rapid manufacturing of metal components by laser forming", *Int. J. Mach. Tools & Manuf.*, vol. 46, pp. 1459–1468, 2006

[5] E. Walner, "Titan- und Nickellegierungen- unverzichtbar im Flugzeugbau", *Ingenieur-Werkstoffe, Konstruktion*, pp. 6-7, May 2008
[6] M. Peters, J. Kumpfert, C.H. Ward, et al., "Titanium alloys for aerospace applications", *Advanced Engineering Materials*, vol. 5, pp. 419-427, 2003
[7] M. Peters and C. Leyens, *Titan und Titanlegierungen,* Weinheim (Germany), Wiley VCH, 2002
[8] J.P. Bergmann, "Laserstrahlschweißen von Titanwerkstoffen unter Berücksichtigung des Einflusses des Sauerstoffes", *Materialwissenschaft und Werkstofftechnik*, vol. 35, n°. 9, pp. 543-556, 2004
[9] J.D. Kim and Y. Peng, "Plunging method for Nd:YAG laser cladding with wire feeding", *Optics and Lasers in Engineering*, vol. 33, n°. 4, pp. 299-309, 2000
[10] W.U.H. Syed and L. Li, "Effects of wire feeding direction and location in multiple layer diode laser direct metal deposition", *Applied Surface Science*, vol. 248, pp. 518-524, 2005
[11] W.U.H. Syed, A.J. Pinkerton and L. Li, "Combined wire and powder feeding laser direct metal deposition for rapid prototyping", 23rd International Congress on Applications of Lasers and Electro-Optics San Francisco (USA), 2004
[12] J.D. Kim, K.H. Kang and J.N. Kim, "Nd:YAG laser cladding of marine propeller with hastelloy c-22", *Appl. Phys.*, vol. A79, pp. 1583-1585, 2004
[13] K.C. Meinert, E.W. Reutzel, R.P. Martukanitz, et al., "Design of weld joints for non-autogenous laser welding of thick sections", International Congress On Applications of Lasers and Electro-Optics, Dearborn (USA), 2000
[14] J. Tusek, M. Hrzenjak, K. Pompe, et al., "Laser repair welding of moulds and dies", proceedings of 5th international conference on industrial tools, Velenje (Slovenia), 2005
[15] L.E. Brown, T.P. Fuesting, J.J. Beaman, et al., "Method and apparatus for making components by direct laser processing", United States, patent US 6,355,086 B2, 12 March 2002
[16] D. Clark, "Laser deposition", United States, patent US 6,989,507 B2, 24 January 2006
[17] S.A. Jones, "Method and apparatus for building up a workpiece by deposit welding", Europe, patent EP 1 245 323 A1, 12 March 2002
[18] I.W. Wright and S.A. jones, "Apparatus and method for forming a body", Europe, patent EP 1 281 467, 5 February 2003
[19] S.A. Jones, "Apparatus and method for forming a body", United States, patent US 2002/139779, 3 November 2002
[20] S.A. Jones, "Apparatus and method for forming a body", United States, patent US 6,825,432 B2, 30 November 2004
[21] R. Milburn, "Method of manufacturing an article", United States, patent US 6,802,122 B2, 12 October 2004
[22] K.H. Stone and N.P. Pearce, "Method and apparatus for building up a workpiece by deposit welding", United States, patent US 6,274,839 B1, 14 August 2001
[23] S.A. Jones and I.W. Wright, "Method of forming a body by free form welding", Europe, patent EP 1 245 322 A1, 2 March 2002
[24] I.W. Wright and S.A. Jones, "Apparatus and method for forming a body", United States, patent US 6,825,433 B2, 30 November 2004
[25] N.N., Rapid Production of Large Aerospace Components, http://www.rapolac.eu/, 20.02.2010
[26] R. Coppinger, "3D welding takes shape", *Flight International*, pp. 27, March 2010
[27] B. Baufeld, O.V.d. Biest and R. Gault, "Additive Manufacturing of Ti-6Al-4V components by shaped metal deposition: microstructure and mechanical properties", *Mat. Des.*, in press 2010
[28] B. Baufeld and O. van der Biest, "Mechanical properties of Ti-6Al-4V specimens produced by shaped metal deposition", *Science and Technology of Advanced Materials*, vol. 10, 18 May 2009
[29] B. Baufeld, O. van der Biest, R. Gault, et al., "Manufacturing Ti-6Al-4V components by shaped metal deposition: microstructure and mechanical properties", Trends in Aerospace Manufacturing (TRAM), Sheffield (UK), IOP Conference Series: Materials Science and Engineering, 2009
[30] B. Baufeld, O. van der Biest and R. Gault, "Microstructure of Ti-6Al-4V specimens produced by shaped metal deposition", *Int. J. Mat. Res.*, vol. 100, pp. 1536-1547, 2009
[31] T. Skiba, B. Baufeld and O. van der Biest, "Microstructure and mechanical properties of stainless steel component manufactured by shaped metal deposition", *IRIJ int.*, vol. 49, pp. 1588-1591, 2009
[32] D. Clark, M.R. Bache and M.T. Whittaker, "Shaped metal deposition of a nickel alloy for aero engine applications", *J. Mat. Proc. Techn.*, vol. 203, pp. 439-448, 2008
[33] SAE Aerospace, "Heat treatment of titanium and titanium alloys", Aerospace Material Specification, AMS-H-81200A, 2003
[34] Deutsche Norm, "Wärmebehandlung von Titan-Knetlegierungen", Deutsches Institut für Normung, DIN 65084, 1990
[35] US department of defense, "Military handbook: titanium and titanium alloys", Department of defense, MIL-H DBK-697A, 1974
[36] C.S.C. Lei, A. Davis and E.W. Lee, "Effect of BSTOA and mill anneal on the mechanical properties of Ti-6Al-4V castings", *Advanced Materials & Processes*, pp. 75-77, May 2000
[37] E.W. Lee, C.S.C. Lei and W.E. Frazier, "Applications, benefits, and implementation of Ti-6Al-4V castings", RTO AVT Specialists' Meeting on "Cost Effective Application of Titanium Alloys in Military Platforms", Loen (Norway), RTO-MP-069(II), 7-11 May 2001

[38] Deutsche Norm, "Metallische Werkstoffe - Zugversuch - Teil 1: Prüfverfahren bei Raumtemperatur", Deutsches Institut für Normung, DIN EN 10002-1, 2001

[39] Deutsche Norm, "Werkstoffprüfung; Dauerschwingversuch, Begriffe, Zeichen, Durchführung, Auswertung", Deutsches Institut für Normung, DIN 50100, 1978

[40] J. Sun and Y.B. Guo, "A comprehensive experimental study on surface integrity by end milling Ti-6Al-4V", *J. Mat. Proc. Techn.*, vol. 209, pp. 4036-4042, 2009

[41] C. Dindorf, "Ermüdung und Korrosion nach mechanischer Oberflächenbehandlung von Leichtmetallen", Dissertation, TU Darmstadt, Fachbereich Material- und Geowissenschaften, 2006

[42] S. Landua, "Einfluss von Gefüge und Schnittgeschwindigkeit auf die Mechanismen der Spanbildung und die Ermüdungseigenschaften von Leichtmetalllegierungen", Dissertation, TU Darmstadt, Fachbereich Material- und Geowissenschaften, 2005

[43] E. Brandl, C. Leyens, C. Dalle Donne, et al., "Deposition of Ti-6Al-4V using Nd:YAG laser & wire: microstructure and mechanical properties", NATO AVT-163 Specialists Meeting on Additive Technology For Repair of Military Hardware, Bonn (Germany), 2009

[44] E. Brandl, C. Leyens and F. Palm, "Mechanical properties of additive manufactured Ti-6Al-4V using wire and powder based processes", Trends in Aerospace Manufacturing (TRAM), Sheffield (UK), IOP Conference Series: Materials Science and Engineering, submitted, 2009

[45] E. Brandl, C. Leyens, F. Palm, et al., "Wire instead of powder? Properties of additive manufactured Ti-6Al-4V for aerospace applications", proceedings of Euro-uRapid, R. Meyer, Berlin, Germany, Fraunhofer Allianz, 2008

[46] SAE Aerospace, "Titanium Alloy Bars, Wire, Forgings, Rings, and Drawn Shapes 6Al - 4V Annealed", Aerospace Material Specification, AMS 4928R, 2007

[47] ASTM International, "standard specification for titanium-6aluminum-4vanadium alloy castings for surgical implants (UNS R56406)", ASTM International, F 1108-04, 2004

[48] G. Welsch, R. Boyer and E.W. Collings, *Materials properties handbook: titanium Alloys, 2nd edition*, Materials Park, Ohio, ASM International, 1998

[49] N.E. Dowling, *Mechanical behavior of materials, Third Edition*, Blacksburg, Virginia, Prentice Hall, 2007

[50] G. Lütjering and J.C. Williams, *Titanium,* Berlin, Heidelberg, New York, Springer, 2003

[51] G. Welsch, W. Bunk and H. Kellerer, "Einfluß von Spannungsfrei-Glühung und Abkühlgeschwindigkeit auf Mikrostruktur und Festigkeit von TiAl6V", *Z. Werkstofftechnik*, Weinheim, Verlag Chemie, vol. 8, n°. 5, pp. 141-149, May 1977

[52] D.-G. Lee, S. Lee and C.S. Lee, "Quasi-static and dynamic deformation behavior of Ti–6Al–4V alloy containing fine alpha$_2$-Ti$_3$Al precipitates", *Materials Science and Engineering*, vol. A366, pp. 25-37, 2004

[53] Y. Murakami, "Phase transformation and heat transport", proceedings of 4th international conference on titanium, H. Kimura and O. Izumi, Kyoto (Japan), pp. 153-167, 19-22 May 1980

[54] H. Kellerer, "Übersicht über die Wärmebehandlung von TiAl6V4", *Härterei-Technische Mitteilungen*, vol. 25, n°. 4, 1970

[55] RMI Titanium, "Facts about the metallography of titanium", Niles (USA), RMI Titanium, 1981

[56] E. Hornbogen and H. Warlimont, *Metallkunde: Aufbau und Eigenschaften von Metallen und Legierungen, 4. Auflage*, Berlin, Springer Verlag, 2000

[57] C. Leyens and M. Peters, *Titanium and titanium Alloys: fundamentals and applications,* Weinheim, Wiley-VCH, 2003

[58] I. Kelbassa, "Qualifizieren des Laserstrahl-Auftragschweißens von BLISKs aus Nickel- und Titanbasislegierungen", Dissertation, RWTH Aachen, 2006

[59] C. Charles, "Modelling microstructure evolution of weld deposited Ti-6Al-4V", Licentiate thesis, Lulea University of Technology (Sweden), Department of Applied Physics and Mechanical Engineering, 2008

[60] P.A. Kobryn and S.L. Semiatin, "Mechanical properties of laser-deposited Ti-6Al-4V", *JOM*, 2006

[61] M. Svensson, "Material properties of EBM-manufactured TI6AL4V & TI6AL4V ELI under raw and hip conditions", Arcam AB (Sweden), 2009

[62] J.C. Williams and E.A. Starke jr., *Deformation, processing, and structure,* Metals Park, OH, American Society of Metals, 1984

[63] US department of defense, *Military handbook: room-temperature design properties,* vol. MIL-HDBK-5H, pp. 9-18 to 9-64, 1998

[64] US department of defense, "Military handbook: alpha-beta titanium alloys", MIL-HDBK-5H, part 5.4, pp. 5-51 to 5-93, 1998

[65] B. Baufeld, O.v.d. Biest and S. Dillien, "Texture and crystal orientation in Ti-6Al-4V builds fabricated by shaped metal deposition", *Met. Mat. Trans. A*, in press 2010

[66] J.C. Williams and G. Lütjering, *Titanium '80 science and technology* H. Kimura and O. Izumi, TMS-AIME, vol. 1, 1981

[67] G.P. Dinda, L. Song and J. Mazumder, "Fabrication of Ti-6Al-4V scaffolds by direct metal deposition", *Met. Mat. Trans.*, vol. 39 A, pp. 2914-2922, December 2008

[68] R.B. Sparks and J.R. Long, "Improved manufacturing methods for producing high integrity more reliable titanium forgings", *AFML-TR-73-301*, February 1974